

# ALPHA MATTER REVISITED

J. W. Clark<sup>1,2</sup> and E. Krotscheck<sup>3,4</sup>

<sup>1</sup>*Centro de Investigação em Matemática e Aplicações,  
University of Madeira, 9020-105 Funchal, Madeira, Portugal*

<sup>2</sup>*Department of Physics, Washington University, St. Louis MO 63130, USA*

<sup>3</sup>*Department of Physics, University at Buffalo, SUNY Buffalo NY 14260 and*

<sup>4</sup>*Institut für Theoretische Physik, Johannes Kepler Universität, A 4040 Linz, Austria*

We examine in detail two alternative descriptions of a system of  $\alpha$  particles interacting via local interactions of different character, highlighting the fact that a faithful microscopic description of such systems demands a consistent treatment of both short- and long-range correlations. In preparation, we examine four different versions of modern microscopic many-body theory and conclude by emphasizing that these approaches, although *a priori* very different, actually lead to the same equations for their efficient application. The only quantity that depends on the formulation of many-body theory chosen is an *irreducible* interaction correction. In the language of Green's functions and Feynman diagrams, it is the set of both particle-particle and particle-hole irreducible diagrams, and in variational Jastrow-Feenberg theory it is determined by *multipartite correlations* and *elementary diagrams*. We apply these theoretical methods to the calculation of the energetics, structure, thermodynamics, and dynamics of  $\alpha$  matter, as well as its condensate fraction. In dimensionless units,  $\alpha$  matter appears to be remarkably similar to the much-studied  ${}^4\text{He}$  quantum fluid, its low-temperature properties now basically solved in the Jastrow-Feenberg framework. Accordingly, one can have confidence in the results of application of the same procedure to  $\alpha$  matter. Even so, closer examination reveals significant differences between the physics of the two systems. Within an infinite nuclear medium, alpha matter is subject to a spinoidal instability. Extended mixtures of nucleons and alpha particles are yet to be given rigorous consideration in a corresponding theoretical framework.

## I. INTRODUCTION

Alpha matter [1–4] was originally conceived as an alternative model of infinitely extended nuclear matter composed of intact  ${}^4\text{He}$  nuclei treated as point bosons interacting via a central two-body potential that fits  $\alpha - \alpha$  scattering data. Immediately, there is the prospect of an intriguing correspondence between such  $\alpha$ -particle matter and its atomic counterpart liquid  ${}^4\text{He}$ , for which the ground-state structure and low-lying excitations are now basically a solved quantum many-body problem. Quite naturally, this correspondence was exploited in an early application of correlated-wave-function theory to  $\alpha$  matter [4], as well as some of the subsequent theoretical investigations of the equation of state and other properties of this hypothetical system, now spanning nearly sixty years [5]–[23].

Among Refs. [1]–[23], theoretical studies of the ground state and other properties of a system involving many interacting  $\alpha$  particles divide roughly into two categories. In the first category, exemplified specifically by Refs. [4, 6, 8] and partially in Ref. [14], effort is made to describe the system at the microscopic level based on  $\alpha - \alpha$  two-body interactions that fit  $\alpha - \alpha$  scattering data to a suitable approximation. This task is carried out by application of one or another of the available brands of first-principles quantum many-body theory that will be surveyed in Sec. II.

The Ali-Bodmer (AB) potential [24] (1966) is the most common choice for the basic two-body  $\alpha - \alpha$  interaction in studies of the ground-state, elementary excitations,

dynamics, and thermodynamic properties of  $\alpha$  matter. With its four parameters chosen to fit scattering data in leading states  $L = 0, 2, 4$  of angular momentum up to 24 MeV, this interaction consists of an  $L$ -dependent inner repulsive gaussian term and an  $L$ -independent outer attractive gaussian term,

$$V^{(L)}(r) = V_R^{(L)} \exp \left[ - \left( \mu_R^{(L)} \right)^2 r^2 \right] - V_A \exp \left[ - \mu_A^2 r^2 \right]. \quad (1.1)$$

Alternative  $\alpha - \alpha$  potential models of comparable quality were developed earlier in the same period, also fitted to low- $L$  scattering. Among them, the version labeled ESH [25] features an inner hard core of  $L$ -dependent radius, plus repulsive and attractive gaussian terms of the same form as in the AB potential. In the studies of  $\alpha$  matter based on true quantum many-body theories beyond a mean-field description, the Ali-Bodmer interaction has generally been adopted as the standard choice for assessment of different microscopic many-body approaches among those methods reviewed in Sec. II.

The second category among theoretical approaches to prediction of the properties of  $\alpha$  matter and  $\alpha$ -nucleon mixtures employs versions of the  $\alpha - \alpha$  interaction *alternative* to the Ali-Bodmer potential, derived by a double-folding procedure applied to Gogny [26, 27] or Skyrme [28] parametrizations of effective *two-nucleon* potentials [14, 16, 17, 19, 20, 22, 23]. These versions are evolved specifically from Gogny-D1 [26] and Gogny-D1N [27] nucleon-nucleon interactions in the case of Ref. [14].

An explicit demonstration of the remarkable similitude of the many-body problems of  $\alpha$  matter and liquid  ${}^4\text{He}$  is

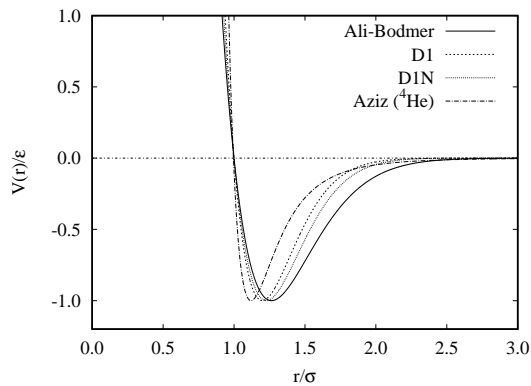


FIG. 1. Aziz interaction [29] for  ${}^4\text{He}$  (dash-dotted line) and Ali-Bodmer interaction [24] (solid line) for  $\alpha$ -matter, in normalized units. Also shown are curves for versions of the  $\alpha - \alpha$  interaction derived from versions D1 and D1N of the Gogny variety of two-nucleon interactions.

provided by Fig. 1. Shown there is a comparison between the Aziz atom-atom interaction [29] in liquid  ${}^4\text{He}$  and three proposed  $\alpha - \alpha$  interactions, namely the Ali-Bodmer  $L = 0$  interaction and the two surrogate  $\alpha - \alpha$  interactions of Ref. [14] derived from Gogny-D1 and Gogny-D1N effective two-nucleon interactions.

The vast difference of scales is accommodated by measuring the separation  $r$  and potential  $V(r)$  in units of the respective values of the range and depth parameters  $\sigma$  and  $\epsilon$  for the two systems. (The range  $\sigma$  is defined as the distance below which the interaction becomes repulsive).

For the four systems, the corresponding values of the deBoer parameter [30],

$$\Lambda = \left( \frac{\hbar^2}{m\epsilon\sigma^2} \right)^{1/2}, \quad (1.2)$$

which is the basis for the quantum law of corresponding states, are listed in Table I.

	Aziz	Ali-Bodmer	D1	D1N
$\sigma$	2.65	2.214	2.819	2.544
$\epsilon$	10.8	11.975	4.620	7.220
$\Lambda$	2.51	2.65	3.35	2.97

TABLE I.

Here we must note that strictly, the deBoer parameter is defined specifically for 6-12 potentials. Still, in the present case it gives a reasonable criterion for comparing interactions and for normalizing associated energetics, in support of the conclusion that  $\alpha$  matter and liquid  ${}^4\text{He}$  are indeed rather similar.

The repulsive strength of the Ali-Bodmer interaction drops from 475 MeV for  $L = 0$  to 320 MeV for  $L = 2$  to 10 MeV for  $L = 4$  [24]. In our calculation of  $\alpha$ -matter properties, we have used only the  $L = 0$  component of this

interaction, acting in all states. Although this simplification overestimates the binding energy somewhat, we will find that use of the more attractive  $L$ -dependent interaction would only lead to more binding and (as will be seen) make the behavior of the model even less realistic with respect to stability.

Our current effort belongs to the first category named above. Sec. II provides an extensive survey of state-of-the-art quantum many-body methods, with specific attention to approaches and aspects that are directly relevant to the microscopic physics of  $\alpha$  matter as a strongly interacting multi-boson system. In particular, attention is given to extended Jastrow-Feenberg theory, parquet-diagrammatics, pair density functions, energetics, consistency, finite-temperature behavior, and dynamics. In Sec. III we present and discuss numerical results for  $\alpha$ -system ground-state energetics and structure, condensate fraction, and dynamics based on Jastrow-Feenberg and parquet theory. Sec. IV concludes with a brief summary of the status of the alpha-matter problem.

While this paper addresses the question of the properties and behavior of pure  $\alpha$ -matter, we do not attempt to solve the problem of how and under what conditions ordinary nuclear matter composed of a soup of nucleons may be subject to the formation of  $\alpha$  clusters, *i.e.* nucleon quartets, or the converse. Such a clustering process, considered at length in several review articles [31–33], is analogous to that of BCS-like pairing in neutron matter [34]. Just as in the BCS case, essential input its theoretical treatment is the interaction that causes quarteting. Microscopic many-body theory derives such an interaction from an underlying microscopic interaction such as variants of the Reid potential [35, 36], the Argonne interaction [37], or more modern interactions based on effective field theories [38, 39]. As we will see in the next section, this task is far less demanding than one might think. True, one has to deal with the complications of Fermi statistics, but these can be handled [40]–[44]. In fact, for the pairing problem, serious microscopic many-body theory has revealed effects that had been overlooked in the past, and it should be quite worthwhile to examine analogous issues for the quarteting problem.

## II. GENERIC MANY-BODY THEORY

Microscopic many-body theory has been developed over numerous decades since the 1950s, initially along very different lines, specifically quantum field theory [45], the Jastrow-Feenberg variational method [46], and coupled-cluster theory [47], applied predominantly to systems of fermions. Here we are interested in a system of identical bosons. With the exception of applications within Jastrow-Feenberg theory, Bose systems have been less well examined, but any method developed for fermions can readily be adapted to bosons by taking the limit where the degree of degeneracy of single-particle states goes to infinity and the Fermi wave number goes

to zero, while keeping the particle density fixed.

Certain simple physical considerations are involved in specifying which effects a satisfactory theoretical description of an interacting many-particle system should contain. These are:

- (i) short-range correlations to describe the influence of the interaction on the wave function as well as saturation, and
- (ii) stability of the system under external perturbations.

Observing these simple criteria, microscopic many-body theory has been developed along different pathways to be described briefly below. Though apparently very different at the outset, in the final analysis these approaches lead, however, to exactly the same set of equations for implementation. This fact prompted the authors of Ref. 48 to conclude that “many-body theory has been developed to a level where different approaches are a matter of language, but not of substance” (see also Ref. [49]). Accordingly, we here use the term *generic many-body theory*.

This situation is completely clear for a system of bosons. Formally, the case of Fermi liquids has been less extensively studied in this respect. The same objectives still apply, but naturally the issues become more complicated because of the multitude of exchange diagrams, and some additional approximations need to be made to establish the equivalence between the Jastrow-Feenberg method and that based on parquet-diagram summations [50].

### A. Jastrow-Feenberg Method

Historically, the first and best-explored approach leading to what we will call generic many-body theory is the Jastrow-Feenberg method. For bosons, the method starts with an *ansatz* for the wave function:

$$|\Psi_0\rangle = \exp \frac{1}{2} \left[ \sum_{i<j} u_2(\mathbf{r}_i, \mathbf{r}_j) + \sum_{i<j<k} u_3(\mathbf{r}_i, \mathbf{r}_j, \mathbf{r}_k) + \dots \right]. \quad (2.1)$$

The correlation functions  $u_n(\mathbf{r}_{i_1}, \dots, \mathbf{r}_{i_n})$  are obtained by minimizing the energy expectation value:

$$E = \frac{\langle \Psi_0 | H | \Psi_0 \rangle}{\langle \Psi_0 | \Psi_0 \rangle}, \quad \frac{\delta E}{\delta u_n}(\mathbf{r}_1, \dots, \mathbf{r}_n) = 0. \quad (2.2)$$

This method is, in principle, exact. Approximations are defined by the number of correlation functions retained and how the so-called “elementary diagrams” are treated, as explained below. The connections to the observable pair distribution function

$$\begin{aligned} g(\mathbf{r}, \mathbf{r}') &= g(|\mathbf{r} - \mathbf{r}'|) \\ &= \frac{1}{\rho^2} \frac{\langle \Psi_0 | \sum_{i \neq j} \delta(\mathbf{r}_i - \mathbf{r}) \delta(\mathbf{r}_j - \mathbf{r}') | \Psi_0 \rangle}{\langle \Psi_0 | \Psi_0 \rangle} \end{aligned} \quad (2.3)$$

and static structure function

$$S(k) = 1 + \rho \int d^3 r e^{i\mathbf{k} \cdot \mathbf{r}} [g(r) - 1] \quad (2.4)$$

are made through the hierarchy of hypernetted chain equations [51, 52]. The variations in Eqs. (2.2) with respect to the correlation functions  $u_n(\mathbf{r}_{i_1}, \dots, \mathbf{r}_{i_n})$  are then re-expressed in terms of the variations with respect to the observable  $g(\mathbf{r} - \mathbf{r}')$  and higher-order  $n$ -body distribution functions,

$$\frac{\delta E}{\delta g_n}(\mathbf{r}_1, \dots, \mathbf{r}_n) = 0. \quad (2.5)$$

This procedure has been described in textbooks [46] and pedagogical material [53]; we highlight here only its most essential features. In practice, stopping at three-body correlations has proven to be sufficient [54–56]. These are dealt with by first optimizing the triplet correlations for fixed pair correlation functions. The result is then inserted into the energy functional, which then only depends on  $g(r)$  and  $S(k)$ . For further reference, we spell out the explicit form:

$$E = E_R + E_I + E_Q, \quad (2.6)$$

where

$$E_R = N \frac{\rho}{2} \int d^3 r \left[ v(r)g(r) + \frac{\hbar^2}{m} \left| \nabla \sqrt{g(r)} \right|^2 \right], \quad (2.7)$$

$$E_Q = -\frac{N}{4} \int \frac{d^3 k}{(2\pi)^3 \rho} t(k) \frac{(S(k) - 1)^3}{S(k)}, \quad (2.8)$$

in which  $t(k) = \hbar^2 k^2 / 2m$  and  $E_I$  is the contribution from elementary diagrams and higher correlation functions  $u_n(\mathbf{r}_1, \dots, \mathbf{r}_n)$  for  $n \geq 3$ . Here,  $E_I$  is a functional of the pair distribution function  $g(r)$  that generates the irreducible interaction through

$$V_I(r) = \frac{2}{\rho} \frac{\delta E_I}{\delta g(r)}. \quad (2.9)$$

Manipulating the Euler equation for  $g(r)$ , one obtains the familiar Bogoliubov formula

$$S(k) = \frac{t(k)}{\epsilon_F(k)} = \left[ 1 + \frac{2}{t(k)} \tilde{V}_{p-h}(k) \right]^{-\frac{1}{2}}, \quad (2.10)$$

where

$$\epsilon_F(k) = \sqrt{t^2(k) + 2t(k)\tilde{V}_{p-h}(k)} = \frac{t(k)}{S(k)} \quad (2.11)$$

is the Feynman dispersion relation [57] and  $\tilde{V}_{p-h}(k)$  is an effective local “particle-hole” interaction. The latter quantity is given in coordinate space by

$$\begin{aligned} V_{p-h}(r) &= g(r) [v(r) + V_I(r)] + \frac{\hbar^2}{m} \left| \nabla \sqrt{g(r)} \right|^2 \\ &\quad + [g(r) - 1] w_I(r), \end{aligned} \quad (2.12)$$

where  $w_I(r)$  is the *induced potential*

$$\tilde{w}_I(k) = -\frac{t(k)}{2} \left[ \frac{1}{S^2(k)} - 1 \right] - t(k) [S(k) - 1]. \quad (2.13)$$

As usual in this field, we have defined the dimensionless Fourier transform by including a particle number density factor  $\rho$ :

$$\tilde{f}(k) \equiv \rho \int d^3r e^{i\mathbf{k}\cdot\mathbf{r}} f(r). \quad (2.14)$$

The correction  $V_I(r)$  in (2.12) comes from the *elementary diagram* contributions, which have to be included term-by-term; they change the numerical values of the results, but not the analytic structure of the equations. Also, three-body correlations lead only to a quantitative modification of that term [56].

A simple rearrangement [58] of Eqs. (2.10) and (2.13) allows us to rewrite the Euler equation in the form

$$\frac{\hbar^2}{m} \nabla^2 \sqrt{g(r)} = V_{p-p}(r) \sqrt{g(r)}, \quad (2.15)$$

with

$$V_{p-p}(r) \equiv v(r) + V_I(r) + w_I(r). \quad (2.16)$$

Eq. (2.15) can be recognized as a boson Bethe-Goldstone equation in terms of an effective particle-particle interaction  $V_{p-p}(r)$ . This observation led Buchler, Sim, and Woo [59] to the conclusion that “...it appears that the optimized Jastrow function is capable of summing all rings and ladders, and partially all other diagrams, to infinite order.”

It is immediately clear that the induced interaction  $w_I(r)$  has non-negligible effect in Eq. (2.15): For  $r \rightarrow \infty$ , the *correct* pair distribution function goes [46] as  $g(r) \sim 1 + \hbar/(2mc_s\rho\pi^2r^4)$ , where  $c_s$  is the hydrodynamic speed of sound. If one leaves out the correlation corrections  $w_I(r)$ , the solution of Eq. (2.15) will behave as  $g(r) \sim 1 + a/r$ , where  $a$  is related to the *S wave scattering length* of the potential. In other words, the correlation corrections to the particle-particle interaction must be just right to guarantee that  $V_{p-p}(r)$  has zero scattering length.

## B. Parquet Diagram Summations

Following up on the observation of Ref. 59, Jackson, Lande, and Smith [48, 60] began with standard Green's function perturbation theory [45, 61]. Arguing that the self-consistent summation of ring- and ladder-diagrams was the minimum requirement for a satisfactory microscopic description of strongly interacting many-particle systems, they carried out the corresponding summations and, what is most important, made the summation practical by introducing local approximations [48, 60].

To summarize this incisive analysis and synthesis, the operative procedure amounts to the following:

- (i) Begin with a local particle-hole interaction, and sum the ring diagrams to obtain

$$\chi(k, \omega) = \frac{\chi_0(k, \omega)}{1 - \tilde{V}_{p-h}(k)\chi_0(k, \omega)}, \quad (2.17)$$

where  $\chi_0(k, \omega)$  is the density-density response function of the non-interacting system, expressed for bosons as

$$\chi_0(k, \omega) = \frac{2t(k)}{(\hbar\omega + i\eta)^2 - t^2(k)}. \quad (2.18)$$

The frequency integration

$$S(k) = - \int_0^\infty \frac{d(\hbar\omega)}{\pi} \text{Im} \chi(k, \omega) \quad (2.19)$$

then leads to the familiar Bogoliubov formula (2.10).

- (ii) Define an *energy-dependent* particle-hole reducible interaction,

$$\tilde{w}_I(k, \omega) = \frac{\tilde{V}_{p-h}(k)}{1 - \tilde{V}_{p-h}(k)\chi_0(k, \omega)}. \quad (2.20)$$

- (iii) Define an *energy-independent* particle-hole reducible interaction  $\tilde{w}_I(k) \equiv \tilde{w}_I(k, \bar{\omega}(k))$  by demanding that its frequency integration gives the same observable  $S(k)$  as the frequency integration obtained with  $\tilde{w}_I(k, \omega)$ ; thus

$$\begin{aligned} & \int_0^\infty d(\hbar\omega) \text{Im} [\chi_0(k, \omega) \tilde{w}_I(k, \omega) \chi_0(k, \omega)] \\ &= \int_0^\infty (d\hbar\omega) \text{Im} [\chi_0(k, \omega) \tilde{w}_I(k, \bar{\omega}(k)) \chi_0(k, \omega)] \end{aligned} \quad (2.21)$$

- (iv) Sum the ladder diagrams with this local interaction to arrive at

$$\frac{\hbar^2}{m} \nabla^2 \psi(r) = [v(r) + w_I(r)] \psi(r), \quad (2.22)$$

noting that  $g(r) = |\psi(r)|^2$  applies as well as Eq. (2.4).

- (v) Finally, construct a local particle-hole irreducible interaction such that the results for  $S(k)$  obtained from Eq. (2.19) and from  $g(r)$  agree.
- (vi) Repeat the process to convergence.

This procedure leads to exactly the same equations (2.10) and (2.15) as before, with the effective interactions (2.12) and (2.13). The only difference is that the correction term  $V_I(r)$  is given by the set of diagrams that are both particle-particle and particle-hole irreducible. The equivalence between Jastrow-Feenberg and parquet diagram summations has been proven to the next order, with the simplest set of totally irreducible diagrams [62] and optimized three-body Jastrow-Feenberg functions again leading to the same answer [63].

### C. Coupled-cluster method

The coupled-cluster method (CCM), originally formulated by Coester and Kümmel [64] and further developed by Bishop and Kümmel, has been very successful in describing electronic systems in condensed matter and chemical settings [65–68]. Somewhat later, CCM has been applied intensively in nuclear physics, where it provides a plausible generalization of the Brueckner-Hartree-Fock method [69–73].

CCM is based on a ground-state ansatz the form [64]

$$|\Psi\rangle = e^{\mathcal{C}}|\Phi_0\rangle, \quad (2.23)$$

in which  $|\Phi_0\rangle$  is a suitable reference state, notably for a Hartree-Fock ground state, while  $\mathcal{C}$  is a cluster operator that generates a linear combination of excited determinants from this ground state. The exponential form ensures size extensivity of the solution. Relatively little has been done with the CCM for strongly interacting Bose systems. In the aftermath of the work on Jastrow-Feenberg and parquet diagram summation and proof of their equivalence, the same issue has been examined within coupled-cluster theory [74]. Importantly, it was established that the so-called “Super-Sub(2)” approximation of the CCM also leads to the same set of equations.

### D. Pair density functional theory

Returning to the variational problems based on Eq. (2.5), it is natural to ask whether a general minimum principle exists for the pair distribution function. In effect, we are seeking a two-body version of the Kohn-Hohenberg [75, 76] theorem.

Following the line of arguments that led to the Kohn-Hohenberg theorem for the one-body density, two statements can be made:

- (i) The kinetic energy  $K$  depends only on  $g(r)$  and not on  $v(r)$ .
- (ii) The total energy has a minimum equal to the ground-state energy at the physical ground-state distribution function. In other words, the ground-state distribution function can be obtained through the variational principle (2.5).

The proof of these results parallels exactly that for the original Kohn-Hohenberg theorem and need not be repeated here. However, in contrast to the formulation of density-functional theory (DFT) where assumptions such as the local-density approximation must be made for the energy functional, more is known about the properties of the pair distribution function, namely:

- (i) The *static structure function* can be derived from a linear-response theory by the usual frequency integration (2.19) from a *local* particle-hole interaction

$V_{p-h}(r)$ . Unlike the three cases above, Eqs. (2.19) and (2.17) are now taken as the *definition* of a local particle-hole interaction consistent with linear-response theory.

- (ii) For small interparticle distances, the wave function should be determined by a two-particle Schrödinger equation

$$-\frac{\hbar^2}{m}\nabla^2\Psi(r)+v(r)\Psi(r) = \lambda\Psi(r), \quad r \rightarrow 0+, \quad (2.24)$$

in a very loose definition of the “pair wave function”  $\Psi(r)$ .

At short distances, the *pair distribution function*  $g(r)$  is proportional to the square of the pair wave function,

$$g(r) \sim |\Psi(r)|^2, \quad r \rightarrow 0+. \quad (2.25)$$

Without loss of generality, we can therefore assume a general equation for the pair distribution of the form (2.15) for *all* distances, where  $V_{p-p}(r)$  is again a *definition* of the particle-particle interaction based on the pair distribution function and, accordingly, completely general.

If we now demand that the two interactions,  $V_{p-h}(r)$  and  $V_{p-p}(r)$ , yield the *same* pair distribution function  $g(r)$ , we are led [77] to the relationships (2.12) and (2.16), with a yet undetermined correction term  $V_1(r)$ . The *new* aspect of this formulation of the theory is the interpretation of the “irreducible” interaction. In their simplest versions, diagrammatic many-body theories start with  $V_1(r) = 0$  and improve upon this approximation by means of diagram expansions [62, 63, 78]. But this is not the point from which we started here. Instead, we have started from two rather general definitions and are, to some extent, at liberty to choose a suitable phenomenological form of the irreducible interaction correction  $V_1(r)$ .

### E. Energy Calculation

In variational theory, the equations for the pair distribution functions are obtained by minimizing the ground-state energy with respect to their variation, in particular via Eq. (2.5) for  $n = 2$ , as described in Section II A. In both the parquet-diagram and pair-DFT formulations, we begin with the equations of motion for the pair distribution function. For this, we must assume *some* prescription for calculation of the irreducible interaction correction for any given potential, pair distribution function, and density. Then we are able to calculate the pair distribution function (or the static structure function) for *any* potential  $\lambda v(r)$  with  $0 < \lambda < 1$ .

The Hellman-Feynman theorem [79, 80] informs us that the ground-state energy can be calculated by coupling-constant integration of the potential energy alone, simply

$$\frac{E}{N} = \frac{\rho}{2} \int d^3r v(r) \int_0^1 d\lambda g_\lambda(r), \quad (2.26)$$

where  $g_\lambda(r)$  is the pair distribution function calculated for a potential strength  $\lambda v(r)$ . The total energy then becomes a functional of  $v(r)$  and  $g(r)$  of the form

$$\frac{E}{N} = \frac{\rho}{2} \int d^3r v(r)g(r) + \frac{K}{N}, \quad (2.27)$$

where  $K$  is the kinetic energy.

Now, replacing  $v(r)$  by  $\lambda v(r)$  in Eq. (2.6) and differentiating with respect to  $\lambda$ , we have

$$\frac{d}{d\lambda} \frac{E}{N} = \frac{\rho}{2} \int d^3r v(r)g_\lambda(r) + \int d^3r \left( \frac{\delta}{\delta g_\lambda} \frac{E}{N} \right) (r) \frac{dg_\lambda(r)}{d\lambda}. \quad (2.28)$$

The second term in Eq. (2.28) vanishes; hence the result for the energy from the coupling constant integration (2.26) is the same as the energy functional. The above derivation also shows that Eq. (2.26) is true not only for the exact ground state, but also for any *approximate* energy functional, as long as the pair distribution function is obtained by minimizing this approximate energy functional.

### F. Consistency

The long-wavelength limit of the structure function  $S(k)$ , and hence of  $\tilde{V}_{p-h}(k)$ , is determined by the hydrodynamic speed of sound  $c_s$ , thus

$$S(k) \sim \frac{\hbar k}{2mc_s} \quad \text{as } k \rightarrow 0+, \quad (2.29)$$

$$\tilde{V}_{p-h}(0+) = mc_s^2. \quad (2.30)$$

The hydrodynamic speed of sound can, on the other hand, be obtained from the equation of state through

$$mc_s^2 = \frac{d}{d\rho} \rho^2 \frac{d}{d\rho} \frac{E}{N} = \rho \frac{d^2}{d\rho^2} \rho \frac{E}{N}. \quad (2.31)$$

However, only an exact theory provides this consistency [81, 82]. In the present case of  $\alpha$  matter we are interested perforce in a density regime that is close to the spinodal density. Accordingly, consistency between Eqs. (2.30) and (2.31) is imperative. We have therefore resorted, as described in Ref. 83, to a semi-phenomenological modification of the triplet correction to  $V_I(k)$  in the long-wavelength regime to ensure this consistency. This does not change the equation of state in a noticeable way.

### G. Finite temperatures

Historically, the first extension of our “generic” treatment of the boson many-body problem to finite temperatures was, once again, formulated within the Jastrow-Feenberg approach [84]. In a rather involved analysis, the entropy, and from that all other thermodynamic quantities of interest, were calculated directly from a density-matrix constructed from the wave function (2.1).

We have indicated above how, at zero temperature, the generic many-body equations can be derived in different ways. The same is true for the extension of the theory to finite temperatures: The idea is basically that the long-range correlations are determined by the low-lying excitations, which are more affected by temperature. On the other hand, short-range correlations are determined by the short-range interparticle interaction, which is temperature independent. It is therefore legitimate to utilize the Bethe-Goldstone equation as a zero-temperature equation in which only the “rungs,” but not the particle-particle “ladder” propagators, are treated at  $T > 0$ . We can then focus on the RPA aspect expressed in (2.17)-(2.18). The procedure required has been implemented within the parquet-diagram summation method [85, 86].

At finite temperature, the connection between the dynamic susceptibility and the dynamic structure function is

$$\begin{aligned} S(k, \omega) &= -\frac{1}{\pi} \frac{1}{1 - \exp(-\hbar\omega/T)} \mathcal{I}m\chi(k, \omega) \\ &= -\frac{1}{2\pi} \frac{e^{\hbar\omega/2T}}{\sinh(\hbar\omega/2T)} \mathcal{I}m\chi(k, \omega), \end{aligned} \quad (2.32)$$

the static structure function being just

$$S(k) = \int_{-\infty}^{\infty} d(\hbar\omega) S(k, \omega). \quad (2.33)$$

For bosons, the frequency integration is simple. One writes (2.17) as

$$\chi(k, \omega) = \frac{2t(k)}{(\hbar\omega + i\eta)^2 - \epsilon_F^2(k)}, \quad (2.34)$$

which yields

$$S(k, T) = \coth \frac{1}{2} \beta \epsilon_F(k) S_0(k), \quad (2.35)$$

where  $S_0(k)$  is given by the expression (2.10), but where  $\tilde{V}_{p-h}(k)$  depends implicitly on the temperature through the pair distribution function.

It is now straightforward to verify that the equations of motion can be obtained from the variational principle for the free energy

$$F[g, n] = E_0 + \sum_{\mathbf{k}} \frac{\hbar^2 k^2}{2mS(k)} n_k (1 + n_k) - TS, \quad (2.36)$$

with  $E_0$  given by Eq. (2.6), noting again that all functions appearing in these expressions are temperature dependent. Here the  $n_k$  are the occupation numbers of the quasiparticle states, while

$$S = \sum_{\mathbf{k}} [(n_k + 1) \ln(n_k + 1) - n_k \ln n_k] \quad (2.37)$$

is the entropy of a Bose system with quasiparticle occupation numbers  $n_k$ . The two independent functions  $g(r)$

(or  $S(k)$ ) and  $n_k$  are determined by the two extremum conditions

$$\frac{\delta F}{\delta g}(r) = 0 \quad \text{and} \quad \frac{\delta F}{\delta n}(k) = 0, \quad (2.38)$$

which have the solutions (2.35) and

$$n_k = \frac{1}{\exp(\beta\epsilon_F(k)) - 1}. \quad (2.39)$$

Considering the free energy now as a function of the scaled interaction  $\lambda v(r)$ , we arrive at

$$\begin{aligned} \frac{dF}{d\lambda} &= \frac{\partial E}{\partial \lambda} + \int d^3r \frac{\delta F}{\delta g}(r) \frac{dg(r)}{d\lambda} + \sum_{\mathbf{k}} \frac{\delta F}{\delta n}(k) \frac{dn_k}{d\lambda} \\ &= N \frac{\rho}{2} \int d^3r v(r) g(r), \end{aligned} \quad (2.40)$$

owing to the two optimization conditions. Hence the energy functional is the result of coupling-constant integration.

## H. Condensate fraction

Given the wave function (2.1) and assuming that the correlations are known, we may now proceed to calculate the full one-body density matrix

$$\begin{aligned} \rho_1(\mathbf{r}, \mathbf{r}') & \quad (2.41) \\ &= N \frac{\int d^3r_2 \dots d^3r_N \Psi_0(\mathbf{r}, \mathbf{r}_2, \dots, \mathbf{r}_N) \Psi_0(\mathbf{r}', \mathbf{r}_2, \dots, \mathbf{r}_N)}{\int d^3r_1 \dots d^3r_N |\Psi_0(\mathbf{r}_1, \dots, \mathbf{r}_N)|^2}. \end{aligned}$$

Cumulant expansions for the density matrix were derived and applied in Refs. [87–89] and full HNC summations carried out in Ref. [90]. More in line with our present approach of eliminating Jastrow-Feenberg type correlation functions in favor of the pair distribution function is reformulation of the relevant integral equations as carried out in Ref. [91]. Taking the limit of a homogeneous system, Eqs. (5.23a)–(5.23c) of that work become

$$\begin{aligned} \Delta X(r) &= \sqrt{g(r)} \exp(\Delta N(r)) - \frac{1}{2}g(r) - \frac{1}{2} - \Delta N(r), \\ \Delta \tilde{N}(k) &= (S(k) - 1)\Delta \tilde{X}(k), \end{aligned} \quad (2.42)$$

with which the condensate fraction is calculated from

$$\begin{aligned} \ln n_c &= 2\Delta \tilde{X}(0+) \\ &- \int \frac{d^3k}{(2\pi)^3 \rho} \Delta \tilde{N}(k) \left[ \Delta \tilde{X}(k) S(k) + S(k) - 1 \right] \\ &+ \frac{1}{4} \int \frac{d^3k}{(2\pi)^3 \rho} \frac{(S(k) - 1)^3}{S(k)}. \end{aligned} \quad (2.43)$$

These equations can be improved by adding elementary-diagram corrections [90], although an extension to three-body and higher-order correlations has, to our knowledge, not been developed.

Some concerns about the validity of HNC-type expansions for the density matrix from the standpoint of parquet-diagram summations have been expressed in Ref. [92]; the issue has not been investigated any further. Also, the formulation (2.43) leaves out triplet and elementary diagram corrections.

## I. Dynamics

The treatment of many-body dynamics has been most extensively studied along the lines of variational theory. One does not need to assume explicitly a Jastrow-Feenberg wave function; it suffices to assume that  $|\Psi_0\rangle$  is the exact many-body wave function or an approximation sufficiently close to it.

A common formulation of most treatments of the dynamics is to give the dynamic wave function a small, time-dependent component

$$|\Psi(t)\rangle = e^{-iE_0 t/\hbar} \frac{e^{\frac{1}{2}\delta U(t)} |\Psi_0\rangle}{\langle \Psi_0 | e^{\frac{1}{2}\delta U^\dagger(t)} e^{\frac{1}{2}\delta U(t)} | \Psi_0 \rangle^{1/2}}, \quad (2.44)$$

where  $|\Psi_0\rangle$  is the ground state and  $\delta U(t)$  is an excitation operator, written for the case of bosons in the form

$$\delta U(t) = \sum_i \delta u_1(\mathbf{r}_i; t) + \sum_{i < j} \delta u_2(\mathbf{r}_i, \mathbf{r}_j; t) + \dots \quad (2.45)$$

The amplitudes  $\delta u_n(\mathbf{r}_1, \dots, \mathbf{r}_n; t)$  are determined by the time-dependent generalization of the Ritz variational principle:

$$\frac{\delta}{\delta u_n(\mathbf{r}_1, \dots, \mathbf{r}_n; t)} \int dt \langle \Psi(t) | H - i\hbar \partial_t | \Psi(t) \rangle = 0. \quad (2.46)$$

This general approach and its extension to Fermi systems [93–95] has been referred to as ‘‘Dynamic Many-Body Theory (DMBT)’’ and provides, to date, the most accurate overall microscopic description of the dynamics of strongly interacting many-body systems.

For infinitesimal perturbations  $\delta U(t)$  of the ground state, one can linearize the equations of motion for  $\delta u_i(\mathbf{r}_i, \dots; t)$ , leading to the density-density response function  $\chi(k, \omega)$ , from which the dynamic structure function follows as  $S(k, \omega) = \text{Im} \chi(k, \omega)$ . Restriction of the excitation operator to one-body fluctuations  $\delta u_1(\mathbf{r}; t)$  leads to the famous Feynman dispersion relation (2.10) [57], whereas a ‘‘backflow’’ choice of  $\delta u_2(\mathbf{r}_i, \mathbf{r}_j; t)$  yields the Feynman-Cohen estimate of  $e_0(k)$ . Unconstrained variation with respect to  $\delta u_1(\mathbf{r}; t)$  and  $\delta u_2(\mathbf{r}_i, \mathbf{r}_j; t)$  gives, in a specific *convolution approximation* for the three- and four-body vertices, the correlated-basis formulation of Jackson and Feenberg [96, 97], which is the boson version of what is known in nuclear physics as ‘‘second RPA (SRPA)’’ [98–102]. A more accurate evaluation of these vertices [103] provides essentially no improvement.

Permitting fluctuations  $\delta u_n(\mathbf{r}_1, \dots, \mathbf{r}_n; t)$  to all orders [104] finally leads to a response function of the form

$$\chi(k, \omega) = \frac{S(k)}{\hbar\omega - \varepsilon_F(k) - \Sigma(k, \hbar\omega)} + \frac{S(k)}{-\hbar\omega - \varepsilon_F(k) - \Sigma(k, -\hbar\omega)}, \quad (2.47)$$

where the self-energy is given by an integral equation

$$\Sigma(k, \hbar\omega) = \frac{1}{2} \int \frac{d^3k_1 d^3k_2}{(2\pi)^3 \rho} \frac{\delta(\mathbf{k} - \mathbf{k}_1 - \mathbf{k}_2) \left| \tilde{V}_3(\mathbf{k}; \mathbf{k}_1, \mathbf{k}_2) \right|^2}{\hbar\omega - \varepsilon_F(k_1) - \Sigma(k_1, \hbar\omega - \varepsilon_F(k_2)) - \varepsilon_F(k_2) - \Sigma(k_2, \hbar\omega - \varepsilon_F(k_1))}, \quad (2.48)$$

in which  $\tilde{V}_3(\mathbf{k}; \mathbf{p}, \mathbf{q})$  is the three-phonon vertex

$$\tilde{V}_3(\mathbf{k}; \mathbf{k}_1, \mathbf{k}_2) = \frac{\hbar^2}{2m} \sqrt{\frac{S(k_1)S(k_2)}{S(k)}} \left[ \mathbf{k} \cdot \mathbf{k}_1 \tilde{X}(k_1) + \mathbf{k} \cdot \mathbf{k}_2 \tilde{X}(k_2) - k^2 \tilde{X}_3(\mathbf{k}, \mathbf{k}_1, \mathbf{k}_2) \right], \quad (2.49)$$

where  $\tilde{X}(k) = 1 - 1/S(k)$  and  $\tilde{X}_3(\mathbf{k}, \mathbf{k}_1, \mathbf{k}_2)$  is the fully irreducible three-phonon coupling matrix element. In the simplest approximation,  $\tilde{X}_3(\mathbf{k}, \mathbf{k}_1, \mathbf{k}_2)$  is replaced by the three-body correlation  $\tilde{u}_3(\mathbf{k}, \mathbf{k}_1, \mathbf{k}_2)$ . This approximation ensures that long-wavelength properties of the excitation spectrum are preserved [105]. The improved calculations mentioned above [103] sum a 3-point integral equation to guarantee satisfaction of exact properties of  $\tilde{X}_3(\mathbf{k}, \mathbf{k}_1, \mathbf{k}_2)$  as  $k \rightarrow 0+$  and of the Fourier transform  $X_3(\mathbf{r}_1, \mathbf{r}_2, \mathbf{r}_3)$  for  $|\mathbf{r}_1 - \mathbf{r}_2| \rightarrow 0$  and  $|\mathbf{r}_1 - \mathbf{r}_3| \rightarrow 0$  [103].

We include these corrections routinely; they have a small but visible effect only for wave vectors between the maxon and the roton. The Correlated Basis Functions Brillouin-Wigner (CBF-BW) approximation [106] is obtained by omitting the self-energy corrections in the energy denominator of Eq. (2.48).

## J. Summary of theory

We have outlined above four different ways to arrive at exactly the same set of basic equations for a strongly interacting many-body system. At this juncture we need to stress the simplicity of the method. All it takes is the iterative solution of Eqs. (2.10)-(2.13) or, alternatively, Eqs. (2.15), (2.16), and (2.13). In particular, both equations (2.10) and (2.15) have been at the center of many-body theory for decades. One simply asks that the induced interaction is determined such that their solution are the same. The only quantity that requires either diagrammatic or phenomenological input is the irreducible interaction correction  $V_I(r)$ . Even the simplest choice,  $V_I(r) = 0$ , recovers about 80 percent of the binding energy in liquid  ${}^4\text{He}$  and, as we shall see, around 90 percent of the binding energy in  $\alpha$  matter.

---

## III. RESULTS

### A. Energetics and Structure

The saturation density (per nucleon) of isospin-symmetric nuclear matter is  $0.160 \text{ fm}^{-3}$  [107], which corresponds to an  $\alpha$ -particle density of  $0.04 \text{ fm}^{-3}$ . As will be seen, the latter value is below both the spinodal density  $0.053 \text{ fm}^{-3}$  and the saturation density of  $0.082 \text{ fm}^{-3}$  of  $\alpha$ -matter as predicted for the Ali-Bodmer potential (cf. Fig. 2). We have also calculated the equation of state for the  $\alpha$ - $\alpha$  interactions generated from the D1 and D1N versions Gogny interactions by the double-folding procedure applied in Ref. 14. The version D1 did not lead to binding; accordingly its results are not shown. Version D1N led to a binding energy per particle of  $-11.4 \text{ MeV}$  at a saturation density of  $0.034 \text{ fm}^{-3}$ , as seen in Fig. 3. While the saturation density is more reasonable, the binding energy is far too small to provide a faithful model for generic nuclear matter.

Information on the reliability of our calculations can be obtained by considering the convergence of the HNC-EL calculations for  $\alpha$  matter. Even the simplest approximation,  $V_I(r) = 0$ , recovers about 90 % of the binding energy at saturation density. Our results in the HNC-EL//0 approximation agree generally quite well with the results of Ref. 10. Presumably due to limited computational resources then available, that early work only missed the fact that HNC-EL//0 has no solution below the spinodal density.

We have already stressed the similarity of alpha matter to  ${}^4\text{He}$ . In fact, one sees here that the convergence of energy calculations is much better than in  ${}^4\text{He}$ , where the HNC-EL//0 approximation recovers only about 75 % of the binding energy [56].

A rather different picture emerges when comparing equations of state expressed in dimensionless units, as suggested by deBoer scaling. According to the values of the respective deBoer parameters  $\Lambda$  (Eq. (1.2) and Table I, the three equations of state should be quite similar

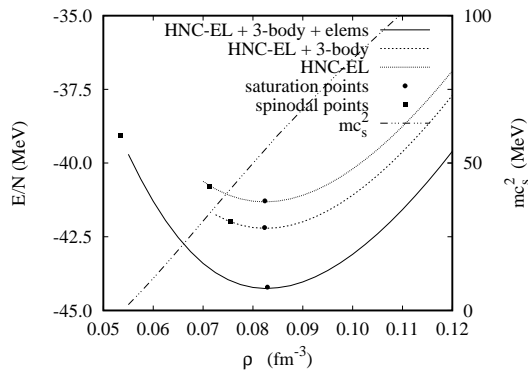


FIG. 2. Comparison between results for the equation of state of alpha matter for the Ali-Bodmer interaction within the HNC framework in HNC-EL//0 approximation as well as when triplets and elementary diagrams are included (left scale). Also shown is the long-wavelength limit, with  $mc_s^2 = \tilde{V}_{p-h}(0+)$  (right scale).

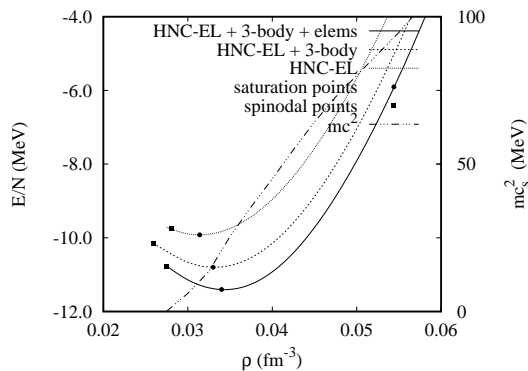


FIG. 3. Same as Fig. 2 but for the D1N interaction.

when expressed in these units. Quite evidently, Fig. 4 shows that they are not. While the scaled orders of magnitude are still comparable,  $\alpha$  matter is much more strongly bound and has a saturation density three times higher. The source of this disparity is the much broader attractive region of the  $\alpha - \alpha$  interactions as compared to the Aziz He-He potential.

For completeness, Figs. 5 and 6 show the pair distribution function and the static structure function obtained for alpha matter as a function of density. Qualitatively, the results are not very different from those for liquid  ${}^4\text{He}$ . However, a remarkable feature of alpha matter is that, unlike the situation in  ${}^4\text{He}$ , the “nearest neighbor peak” in both  $g(r)$  and  $S(k)$  seems to *decrease* as a function of density, indicating that, remarkably, the system becomes *more strongly correlated* when the density is lowered.

We conclude this section with a comment on the importance of “beyond parquet” corrections that are represented by the interaction correction  $V_I(r)$  and the energy correction  $E_I$ . We have seen above that already

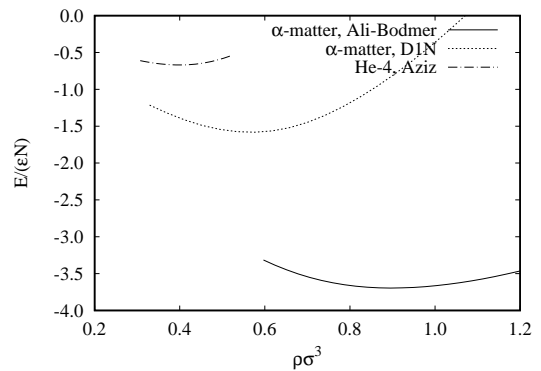


FIG. 4. Comparison of Ali-Bodmer (solid line) and D1N (dashed line) equations of state for alpha matter with that of liquid  ${}^4\text{He}$  for the Aziz interaction (dash-dotted line), in dimensionless units, energy in units of potential depth  $\epsilon$ , and lengths in units of core size  $\sigma$ .

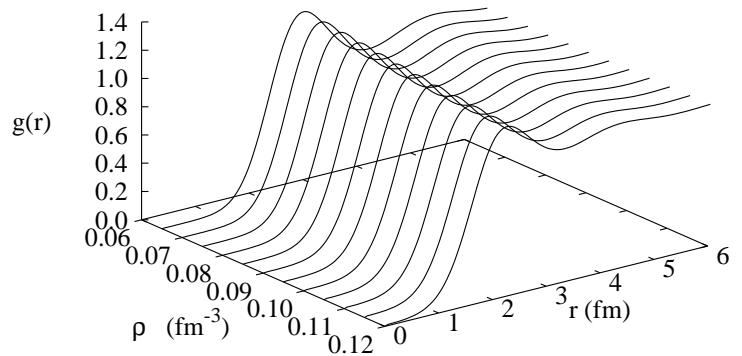


FIG. 5. Pair distribution function  $g(r)$  as a function of density  $\rho$  for the Ali-Bodmer interaction.

the simplest approximation,  $E_I = 0$ , gives a very good prediction for the ground-state energy. Caution should be exercised, however, when generalizing that statement to other quantities. The error in the energy, or, more generally the error in all quantities that follow from a variational principle, is *quadratic* in the deviation of the approximate wave function from the exact one. This applies to all quantities considered here *except*, as we shall see, the condensate fraction, which depends sensitively on the pair distribution function.

Figs. 7 and 8 show three different approximations to the pair distribution function  $g(r)$  for the Ali-Bodmer potential. It was necessary to go to rather high density,  $\rho = 0.07 \text{ fm}^{-3}$ , because the HNC-EL//0 approximation has no solution at lower densities.

An interesting feature is seen in the particle-hole interaction, which again sets  $\alpha$ -matter apart from  ${}^4\text{He}$ . Phenomenologically it is argued [108] that in liquid  ${}^4\text{He}$  the quantity  $V_{p-h}(r)$  (called the “pseudopotential” by Aldrich and Pines) should display:

- (i) an enhancement of the short-distance repulsion due

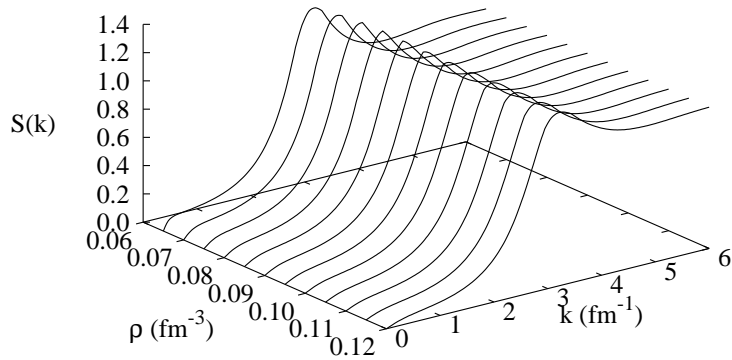


FIG. 6. Static structure function  $S(k)$  as a function of density  $\rho$  for the Ali-Bodmer interaction.

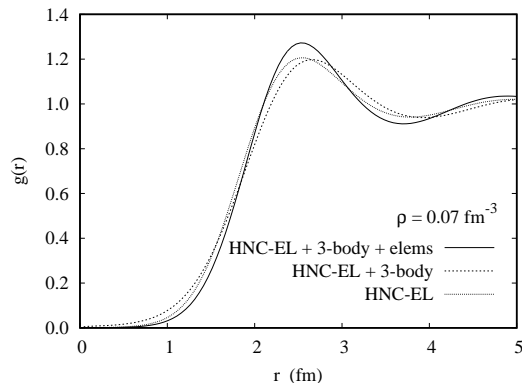


FIG. 7. Pair distribution function  $g(r)$  at the density  $\rho = 0.07 \text{ fm}^{-3}$ , for the Ali-Bodmer interaction. The solid line shows the result including 3-body and elementary-diagram corrections; the dashed line, the result including only 3-body correlations; and the dotted line, the HNC-EL//0 approximation.

to the cost in kinetic energy for bending the wave function to zero at small interparticle distances, and

- (ii) an enhanced attraction at the potential minimum due to the presence of neighboring attractive particles.

In contrast to  ${}^4\text{He}$  where these effects are faithfully reproduced, they are not seen in our results for  $\alpha$ -matter.

## B. Finite Temperature

Results for our calculations at finite temperature are shown in Figs. 9 and 10. We have limited these calculations to the regime  $0 \leq k_B T \leq 10 \text{ MeV}$ , because the theory formulated in section II G assumes a Feynman spectrum that has a roton minimum between 30 and 40 MeV, whereas the best prediction for the collective excitations suggests a roton minimum of 20 to 30 MeV. (See Subsection III D.) Experience from  ${}^4\text{He}$  indicates that rotons

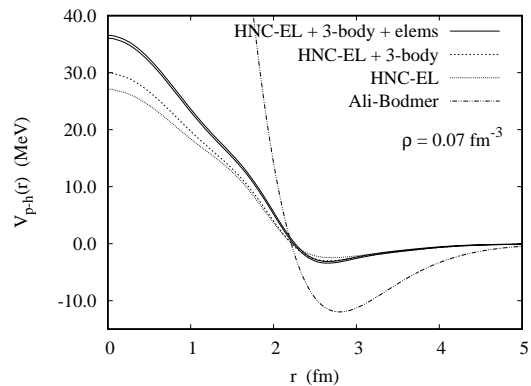


FIG. 8. Same as in Fig. 7, but for the particle-hole interaction  $V_{p-h}(r)$ . The two solid lines show  $V_{p-h}(r)$  when the semi-phenomenological modifications discussed in Section II F are respectively included or omitted. Also shown is the bare Ali-Bodmer potential (dash-dotted line).

already contribute visibly to the thermodynamics of the system at about a tenth of the roton energy [109]; for a quantitative analysis, see Fig. 50 of Ref. 110.

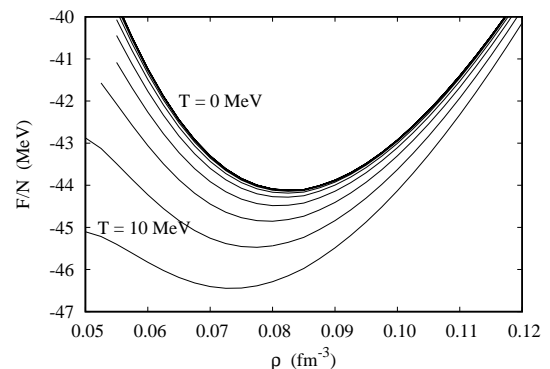


FIG. 9. Free energy  $F/N$  per particle for the Ali-Bodmer interaction in the temperature range  $k_B T = 0, 1, \dots, 10 \text{ MeV}$ .

An interesting feature that sets  $\alpha$ -matter apart from the otherwise rather similar  ${}^4\text{He}$  fluid is that, within the temperature regime studied, we did not observe a significant change of the spinodal density, whereas in  ${}^4\text{He}$  [111] this feature is already observed at 4 K. There is a slight bending of the spinodal line toward lower densities above 10 MeV, but we did not pursue that behavior any further. Improvements of the finite-temperature theory [112] lead to the replacement of the Feynman spectrum by the one predicted by (CBF-BW) approximation [106].

## C. Condensate fraction

Results for the condensate fraction  $n_c$  of Eq. (2.43) are shown in Fig. 11. One can improve upon this calcu-

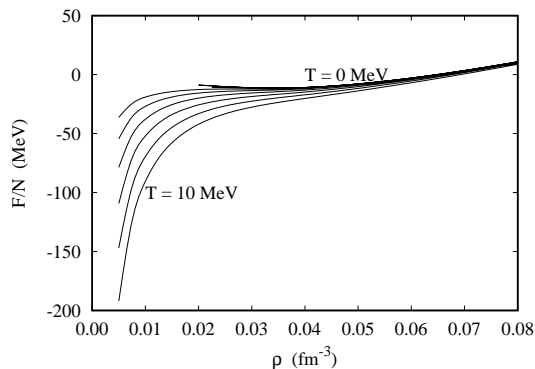


FIG. 10. Same as Fig. 9, but for the D1N interaction. Note that the fact that the higher-temperature curves of  $F/N$  are concave does not contradict the stability condition  $mc_s^2 > 0$ , since  $\rho F/N$  must be convex (see Eq. (2.31)).

lation by including irreducible “elementary-” or “triplet correlation-” diagram corrections in Eq. 2.43. We have deliberately not included these corrections, in order to demonstrate the sensitive dependence of the results on the input pair correlation function.

The results for the Ali-Bodmer interaction are in reasonable agreement with those of Ref. 14, although the latter work uses rather simple cluster expansions and correlation functions. We also show results for the cases where elementary diagrams and/or three-body correlations are omitted. Obviously, the results are quite different and underscore our statement above on the sensitive dependence of the condensate fraction on the input data. For example, one may compare the results in Fig. 7 with the values of  $n_c$  at the same density. Our results do not agree well with those of Ref. 14 for the D1N interaction. Evidently, the reason for this disagreement also lies in the fact that the condensate fraction depends sensitively on the pair correlation function.

The expected accuracy of our results is therefore similar to that of the energy calculation. One can also judge their accuracy by comparing HNC-type calculations [113] for  ${}^4\text{He}$  with corresponding Monte Carlo calculations [114–116], although the correlation functions of Ref. 113 were also non-optimized.

#### D. Dynamics

Implementation of the method outlined only briefly in section III has led to an unprecedented agreement between theoretical predictions [104] and experimental results [110, 117] in  ${}^4\text{He}$ . A small quantitative improvement can be obtained by including 4-body CBF corrections [118]; these have not been included in the present application. The quantity of most immediate interest is the phonon dispersion relation  $e_0(k)$ , which is given by the pole of the density-density response function (2.47). Our results for a sequence of densities around the equi-

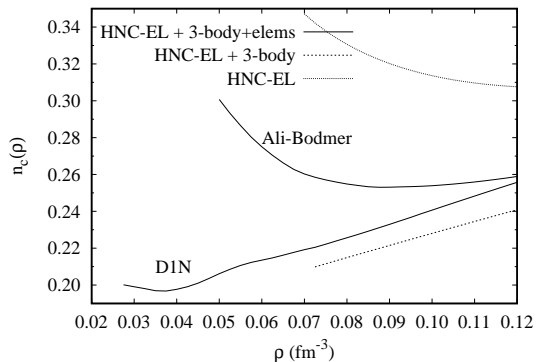


FIG. 11. Condensate fraction of  $\alpha$ -matter as a function of density. The reference to “3-body and elems” refers to the input function  $g(r)$ , but no three-body correlations or elementary diagrams were retained in the explicit expression, *i.e.* Eqs. (2.42) and (2.43) have been used for all calculations. The labeled solid lines depict the most complete calculations for the two interactions considered in this work; simpler versions for the D1N interaction are not shown.

librium density for the Ali-Bodmer interaction are shown in Fig. 12. A feature that immediately distinguishes our results for  $\alpha$  matter from those for  ${}^4\text{He}$  is that both the energy of the roton minimum and that of the maxon are found to *increase* rather than decrease with density. This behavior consistent with the fact, pointed out above, that the behavior of the nearest-neighbor peak in  $g(r)$  also indicates that the lower-density system is more strongly correlated.

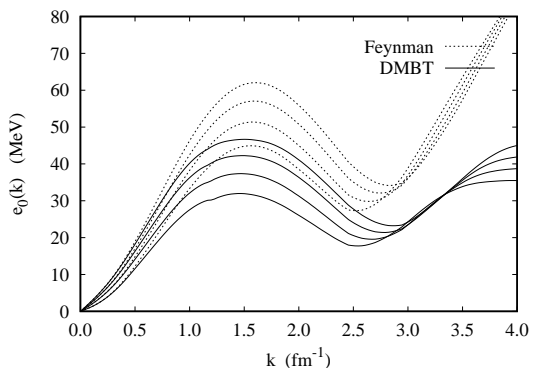


FIG. 12. Zero-sound dispersion relation  $e_0(k)$  for the Ali-Bodmer interaction in Feynman approximation (long-dashed lines), and DMBT [104] (solid lines), for the densities  $\rho = 0.06, 0.07, 0.08, 0.09 \text{ fm}^{-3}$ . The highest density corresponds to the highest roton minimum.

Our results for the D1N interaction shown in Fig. 13 basically support these results. The “roton minimum” appears at a somewhat larger wave length, which is expected because the equilibrium density is substantially lower.

The phonon-roton dispersion relation is only a part of

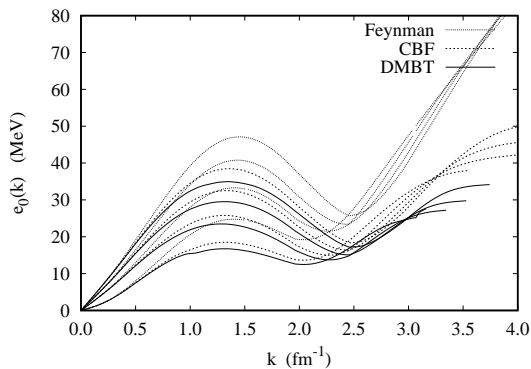


FIG. 13. Same as Fig. 12, but for the D1N interaction and densities  $\rho = 0.03, 0.04, 0.05, 0.06 \text{ fm}^{-3}$ . The highest density corresponds to the highest roton minimum.

the story: From the fact that we are close to the spinodal point we can conclude that the phonon dispersion relation is anomalous, which has the consequence that the phonon has a finite width. Moreover, the existence of a typical phonon-maxon-roton structure has the consequence that for larger momentum transfers, there should be a “Pitaevskii Plateau” [119]. All of these features are seen in the contour plots shown in Figs. 14 and 15. In fact, some of the features exhibited, such as the extension of the plateau to long wavelengths and the extension of the  $R_+$  roton to higher energies as well as its Cherenkov damping, are seen more clearly than in  $^4\text{He}$ .

Fig. 15 provides the same information for the D1N interaction. At the lowest densities,  $S(k, \omega)$  exhibits a remarkably rich structure at high energies, which can be attributed to mode-mode couplings.

We conclude this section by commenting on what is achieved by going beyond the CBF approximation. In that treatment, the energy denominator in the self-energy (2.48) contains only the Feynman spectrum  $\varepsilon_F(k)$ . As a consequence, “mode-mode” couplings would describe only the coupling between Feynman phonons. The most obvious consequence of this restriction is that the so-called “Pitaevskii-plateau,” caused by the fact that it is kinematically permitted for a perturbation to decay into two rotons, appears at twice the roton energy of the Feynman spectrum. A less obvious consequence is that the area above the zero-sound spectrum is filled by a continuum.

#### IV. CONCLUSIONS

We have in this work examined the properties of a fictitious system of  $\alpha$  particles interacting via a local two-body interaction based on scattering data as well as two versions of the  $\alpha - \alpha$  interaction developed from Gogny models of the two-nucleon interaction. We have treated the problem as an exercise of modern microscopic quantum many-body theory, from which much can be learned

with relative ease, as in the case of liquid  $^4\text{He}$ , given its boson constituents. In doing so, we have stressed the fact that four *a-priori* rather different many-body methods, when developed to a level that they contain the same physics, actually lead to the same equations to be solved. These equations are, in fact, quite simple for bosons. The only quantity that must be determined by either diagrammatic expansion or phenomenological considerations is the “totally irreducible” interaction  $V_I(r)$ . We have chosen here the route suggested by Jastrow-Feenberg theory because the derivation of the relevant quantities is then by far the simplest. The parquet-diagram summations lead, to the extent that has been determined so far [62], to the same answer [63].

We have highlighted the similarity of alpha matter to the far better understood system of liquid  $^4\text{He}$ , but we have also exposed its significant differences. From experience with the latter system, we are confident that practically all of the results presented here are quantitative, the only exception being those for the condensate fraction. The phase diagram of  $\alpha$  matter should be very similar to that of  $^4\text{He}$  [120] displaying a spinodal decomposition at low densities, a  $\lambda$  transition from a superfluid to a normal liquid and (with the caveat that model *per se* may be invalid at high densities, a liquid-solid phase transition. In particular there is no indication that  $\alpha$ -particles could form a Bose-Einstein condensate as found in ultracold gases.

It is rather straightforward to extend the calculations to  $\alpha$  droplets, if that should be of interest, in analogy with the case of  $^4\text{He}$  droplets [121–124]. However, the far more relevant problem is that of  $\alpha$ -nucleon mixtures, a fermionic-bosonic composite, whose treatment could follow much the same pattern within the Feenberg-Jastrow framework. See Ref. [22] for a mean-field treatment of this problem. Variational/parquet theory is available for boson-fermion mixtures [63], as well as for realistic nucleon-nucleon interactions [35–37] [40, 41], though necessarily more laborious due to the fermion statistics.

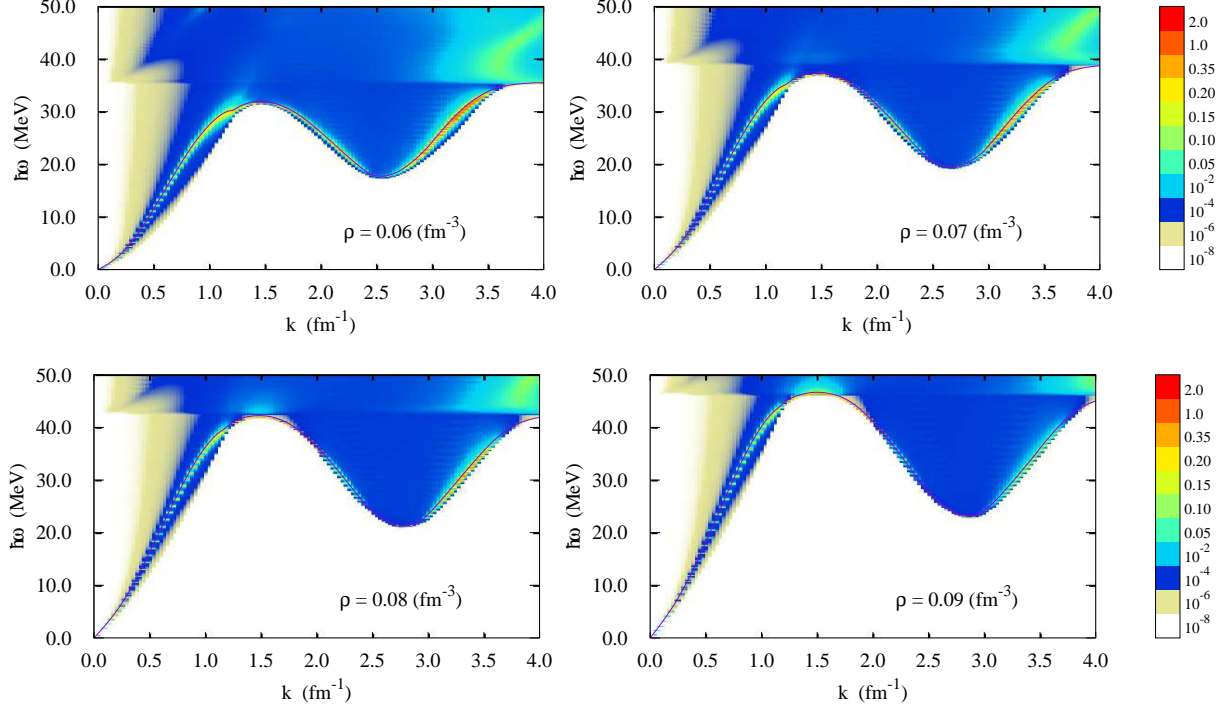


FIG. 14. (color online) Maps of  $S(k, \omega)$  for the Ali-Bodmer potential for a sequence of densities  $\rho = 0.06 \text{ fm}^{-3}, \dots, \rho = 0.09 \text{ fm}^{-3}$ . The solid red line is the phonon dispersion relation, also shown in Fig. 12.

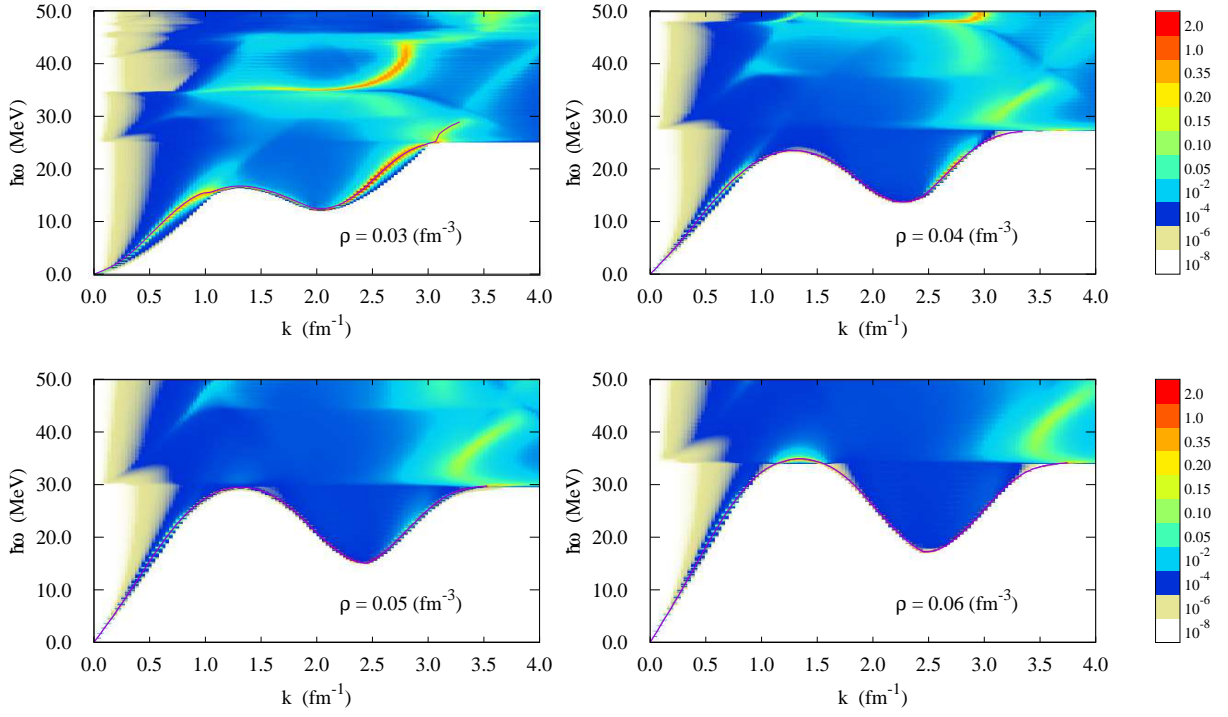


FIG. 15. (color online) Same as Fig. 14 for the D1N interaction and a sequence of densities  $\rho = 0.03 \text{ fm}^{-3}, \dots, \rho = 0.06 \text{ fm}^{-3}$ .

- 
- [1] R. Tamagaki, Prog. Theor. Phys. **29**, 665 (1962).
- [2] M. Nagasaki, Prog. Theor. Phys. **29**, 415 (1963).
- [3] M. Harada, R. Tamagaki, and H. Tanaka, Prog. Theor. Phys. **29**, 933 (1963).
- [4] J. W. Clark and T. P. Wang, Annals of Physics **40**, 127 (1966).
- [5] K. M. Khanna, J. Phys. Soc. Japan **23**, 1429 (1967).
- [6] G. P. Mueller and J. W. Clark, NPA **155**, 561 (1970).
- [7] K. M. Khanna and D. Jairath, Czechoslovak Journal of Physics **26**, 741 (1976).
- [8] J. W. Clark and M. T. Johnson, AIP Conf. Proc. **47**, 544 (1978).
- [9] V. C. Aguilera-Navarro, R. Berrera, J. W. Clark, M. de Llano, and A. Plastino, Phys. Lett. B **80**, 327 (1979).
- [10] M. T. Johnson and J. W. Clark, Kinam **2**, 3 (1980).
- [11] H.-M. Müller and K. Langanke, Phys. Rev. C **49**, 524 (1994).
- [12] A. Sedrakian, H. Müther, and P. Schuck, Nucl. Phys. A **776**, 97 (2006).
- [13] P. Schuck, Y. Funaki, H. Horiuchi, G. Röpke, A. Toshaki, and T. Yamada, Prog. Part. Nucl. Phys. **59**, 285 (2007).
- [14] F. Carstoiu and Ş. Mişicu, Phys. Lett. B **682**, 33 (2009).
- [15] F. Carstoiu and Ş. Mişicu, AIP Conf. Proc. **1304**, 144 (2010).
- [16] F. Carstoiu and Ş. Mişicu, Int. J. Mod. Phys. E **20**, 885 (2010).
- [17] F. Carstoiu, Ş. Mişicu, V. Balanica, and M. Lassault, Rom. J. Phys. **55**, 933 (2010).
- [18] Ş. Mişicu, I. N. Mishustin, and W. Greiner, Int. J. Mod. Phys. Lett. A **32**, 170010 (2016), baryonic matter.
- [19] L. M. Satarov, I. N. Mishustin, A. Mototnenko, V. Vorchenko, M. I. Gorenstein, and H. Stoecker, J. Phys. G. **44**, 125102 (2017).
- [20] L. M. Satarov, I. N. Mishustin, A. Motornenko, V. Vovchenko, M. I. Gorenstein, and H. Stoecker, Phys. Rev. C **99**, 024909 (2019).
- [21] Z.-W. Zhang and L.-W. Chen, Phys. Rev. C **100**, 054304 (2019).
- [22] L. M. Satarov, M. I. Gorenstein, I. N. Mishustin, and H. Stoecker, Phys. Rev. C **101**, 024913 (2020).
- [23] L. M. Satarov, R. V. Poberezhnyuk, I. N. Mishustin, and H. Stoecker, Phys. Rev. C **103**, 024301 (2021).
- [24] S. Ali and A. R. Bodmer, Nucl. Phys. A **80**, 99 (1966).
- [25] O. Endō, I. Shimodaya, and J. Hiura, Prog. Theor. Phys. **31**, 1157 (1964).
- [26] J. Dechargé and D. Gogny, Phys. Rev. C **21**, 1568 (1980).
- [27] F. Chappert, M. Girod, and S. Hilaire, Phys. Lett. B **668**, 420 (2008).
- [28] S. Goriely, N. Chamel, and J. M. Pearson, Phys. Rev. C **82**, 035804 (2010).
- [29] R. A. Aziz, V. P. S. Nain, J. C. Carley, W. J. Taylor, and G. T. McConville, J. Chem. Phys. **70**, 4330 (1979).
- [30] J. D. Boer, Physica **14**, 139 (1948).
- [31] Y. T. Y. Funaki, H. Horiuchi, G. Röpke, P. Schuck, and A. Toshaki, in *Clusters in Nuclei*, Lecture Notes in Physics, Vol. 2 (Springer Verlag, Berlin Heidelberg New York, 2012) pp. 229–298.
- [32] P. Schucki, Y. Funaki, H. Horiuchi, G. Röpke, A. Toshaki, and T. Yamada, Physica Scripta **91**, 123001 (2016).
- [33] G. Röpke, A. Schnell, P. Schuck, and P. Nozières, Phys. Rev. Lett. **80**, 3177 (1998).
- [34] R. Broglia and V. Zelevensky, *Fifty Years of Nuclear BCS* (World Scientific, Singapore, 2013).
- [35] R. V. Reid, Jr., Ann. Phys. (NY) **50**, 411 (1968).
- [36] V. G. J. Stoks, R. A. M. Klomp, C. P. F. Terheggen, and J. J. de Swart, Phys. Rev. C **49**, 2950 (1994).
- [37] R. B. Wiringa, V. G. J. Stoks, and R. Schiavilla, Phys. Rev. C **51**, 38 (1995).
- [38] E. Epelbaum, H.-W. Hammer, and U.-G. Meißner, Rev. Mod. Phys. **81**, 1773 (2009).
- [39] R. Machleidt and D. R. Entern, Physics Reports **500**, 1 (2011).
- [40] E. Krotscheck and J. Wang, Phys. Rev. C **101**, 065804 (2020).
- [41] E. Krotscheck and J. Wang, Phys. Rev. C **102**, 064305 (2020), arXiv:2009.10849.
- [42] E. Krotscheck and J. Wang, Phys. Rev. C **103**, 035808 (2021), arXiv:2010.13194.
- [43] E. Krotscheck and J. Wang, Phys. Rev. C **105**, 034345 (2022).
- [44] E. Krotscheck, P. Papakonstantinou, and J. Wang, arXiv:2308.00873 (2023).
- [45] G. Baym and L. P. Kadanoff, Phys. Rev. **124**, 287 (1961).
- [46] E. Feenberg, *Theory of Quantum Fluids* (Academic Press, New York, 1969).
- [47] H. Kümmel, K. H. Lührmann, and J. G. Zabolitzky, Physics Reports **36**, 1 (1978).
- [48] A. D. Jackson, A. Lande, and R. A. Smith, Physics Reports **86**, 55 (1982).
- [49] A. D. Jackson and T. Wettig, Physics Reports , 1 (1993).
- [50] H.-H. Fan and E. Krotscheck, Physics Reports **823**, 1 (2019).
- [51] T. Morita, Progr. Theor. Phys. **20**, 920 (1958).
- [52] J. M. J. van Leeuwen, J. Groeneveld, and J. D. Boer, Physica **25**, 792 (1959).
- [53] A. Fabrocini, S. Fantoni, and E. Krotscheck, *Introduction to Modern Methods of Quantum Many-Body Theory and their Applications*, Advances in Quantum Many-Body Theory, Vol. 7 (World Scientific, Singapore, 2002).
- [54] C. E. Campbell, Phys. Lett. A **44**, 471 (1973).
- [55] C. C. Chang and C. E. Campbell, Phys. Rev. B **15**, 4238 (1977).
- [56] E. Krotscheck, Phys. Rev. B **33**, 3158 (1986).
- [57] R. P. Feynman, Phys. Rev. **94**, 262 (1954).
- [58] L. J. Lantto and P. J. Siemens, Phys. Lett. B **68**, 308 (1977).
- [59] H. K. Sim, C.-W. Woo, and J. R. Buchler, Phys. Rev. A **2**, 2024 (1970).
- [60] A. D. Jackson, A. Lande, and R. A. Smith, Phys. Rev. Lett. **54**, 1469 (1985).
- [61] A. L. Fetter and J. D. Walecka, *Quantum Theory of Many-Particle Systems* (McGraw-Hill, New York, 1971).
- [62] A. D. Jackson, A. Lande, R. W. Guitink, and R. A. Smith, Phys. Rev. B **31**, 403 (1985).

- [63] E. Krotscheck and M. Saarela, *Physics Reports* **232**, 1 (1993).
- [64] F. Coester and H. Kümmel, *Nucl. Phys.* **17**, 477 (1960).
- [65] R. F. Bishop and K. H. Lüthmann, *Phys. Rev. B* **17**, 3757 (1978).
- [66] R. F. Bishop and K. H. Lüthmann, *Phys. Rev. B* **26**, 5523 (1982).
- [67] R. J. Bartlett and M. Musial, *Rev. Mod. Phys.* **79**, 291 (2007).
- [68] I. Shavitt and R. J. Bartlett, *Many-body methods in chemistry and physics: MBPT and coupled-cluster theory*, Cambridge molecular science series (Cambridge University Press, Cambridge, 2009).
- [69] B. D. Day, *Rev. Mod. Phys.* **50**, 495 (1978).
- [70] B. D. Day, *Phys. Rev. C* **24**, 1203 (1981).
- [71] B. D. Day and J. G. Zabolitzky, *Nucl. Phys. A* **366**, 221 (1981).
- [72] G. Hagen, T. Papenbrock, D. J. Dean, and M. Hjorth-Jensen, *Phys. Rev. C* **82**, 034330 (2010).
- [73] G. Hagen, T. Papenbrock, A. Ekström, K. A. Wendt, G. Baardsen, S. Gandolfi, M. Hjorth-Jensen, and C. J. Horowitz, *Phys. Rev. C* **89**, 014319 (2014).
- [74] R. F. Bishop, in *Condensed Matter Theories*, Vol. 10, edited by M. Casas, J. Navarro, and A. Polls (Nova Science Publishers, Commack, New York, 1995) pp. 483–508.
- [75] P. Hohenberg and W. Kohn, *Phys. Rev. B* **136**, 864 (1964).
- [76] M. Levy, *Proc. Natl. Acad. Sci. USA* **76**, 6062 (1979).
- [77] E. Krotscheck, *Phys. Lett. A* **190**, 201 (1994).
- [78] C. E. Campbell, in *Progress in Liquid Physics*, edited by C. A. Croxton (Wiley, London, 1977) Chap. 6, pp. 213–308.
- [79] H. Hellmann, *Z. Physik* **85**, 180 (1933).
- [80] R. P. Feynman, *Phys. Rev.* **56**, 340 (1939).
- [81] E. Krotscheck, *Phys. Rev. A* **15**, 397 (1977).
- [82] A. D. Jackson and R. A. Smith, *Phys. Rev. A* **36**, 2517 (1987).
- [83] C. E. Campbell, R. Folk, and E. Krotscheck, *J. Low Temp. Phys.* **105**, 13 (1996).
- [84] C. E. Campbell, K. E. Kürten, M. L. Ristig, and G. Senger, *Phys. Rev. B* **30**, 3728 (1984).
- [85] A. Lande and R. A. Smith, (1985), private communication to T. Chakraborty.
- [86] T. Chakraborty, A. Kallio, and M. Puoskari, *Phys. Rev. B* **33**, 635 (1986).
- [87] M. L. Ristig, P. M. Lam, and J. W. Clark, *Phys. Lett. A* **55**, 101 (1975).
- [88] P. M. Lam and C. C. Chang, *Phys. Lett. A* **59**, 356 (1976).
- [89] M. L. Ristig and J. W. Clark, *Phys. Rev. B* **14**, 2875 (1976).
- [90] S. Fantoni, *Nuovo Cimento* **44A**, 191 (1978).
- [91] E. Krotscheck, *Phys. Rev. B* **32**, 5713 (1985).
- [92] T. Wettig and A. D. Jackson, *Phys. Rev. B* **53**, 818 (1996).
- [93] H. M. Böhm, R. Holler, E. Krotscheck, and M. Panholzer, *Phys. Rev. B* **82**, 224505 (2010).
- [94] H. Godfrin, M. Meschke, H.-J. Lauter, A. Sultan, H. M. Böhm, E. Krotscheck, and M. Panholzer, *Nature* **483**, 576 (2012).
- [95] E. Krotscheck and T. Lichtenegger, “Dynamic many body theory IV: (Spin-)density fluctuations and ex-  
change in normal-liquid  $^3\text{He}$ ,” (2022), in preparation.
- [96] H. W. Jackson and E. Feenberg, *Ann. Phys. (NY)* **15**, 266 (1961).
- [97] H. W. Jackson and E. Feenberg, *Rev. Mod. Phys.* **34**, 686 (1962).
- [98] J. Sawicki, *Phys. Rev.* **126**, 2231 (1962).
- [99] C. Yannouleas, M. Dworzecka, and J. J. Griffin, *Nucl. Phys. A* **397**, 239 (1983).
- [100] C. Yannouleas, *Phys. Rev. C* **35**, 1159 (1987).
- [101] J. Wambach, *Reports on Progress in Physics* **51**, 989 (1988).
- [102] P. Papakonstantinou and R. Roth, *Phys. Rev. C* **81**, 024317 (2010).
- [103] C. E. Campbell and E. Krotscheck, *Phys. Rev. B* **80**, 174501 (2009).
- [104] C. E. Campbell, E. Krotscheck, and T. Lichtenegger, *Phys. Rev. B* **91**, 184510/1 (2015).
- [105] C. C. Chang and C. E. Campbell, *Phys. Rev. B* **13**, 3779 (1976).
- [106] H. W. Jackson, *Phys. Rev. A* **8**, 1529 (1973).
- [107] A. Akmal, V. R. Pandharipande, and D. G. Ravenhall, *Phys. Rev. C* **58**, 1804 (1998).
- [108] C. H. Aldrich and D. Pines, *J. Low Temp. Phys.* **25**, 677 (1976).
- [109] L. D. Landau and E. M. Lifshitz, *Statistical Physics, Course of Theoretical Physics*, Vol. V (Pergamon Press Ltd., London - Paris, 1958).
- [110] H. Godfrin, K. Beauvois, A. Sultan, E. Krotscheck, J. Dawidowski, B. Fåk, and J. Ollivier, *Phys. Rev. B* **103**, 104516 (2021), arXiv:2009.10849.
- [111] G. Senger, M. L. Ristig, K. E. Kürten, and C. E. Campbell, *Phys. Rev. B* **33**, 7562 (1986).
- [112] B. E. Clements, E. Krotscheck, J. A. Smith, and C. E. Campbell, *Phys. Rev. B* **47**, 5239 (1993).
- [113] E. Manousakis, V. R. Pandharipande, and Q. N. Usmani, *Phys. Rev. B* **31**, 7022 (1985).
- [114] J. Boronat, in *Microscopic Approaches to Quantum Liquids in Confined Geometries*, edited by E. Krotscheck and J. Navarro (World Scientific, Singapore, 2002) pp. 21–90.
- [115] S. Moroni and M. Boninsegni, *J. Low Temp. Phys.* **136**, 129 (2004).
- [116] R. Rota and J. Boronat, *J. Low Temp. Phys.* **166**, 21 (2011).
- [117] K. Beauvois, C. E. Campbell, J. Dawidowski, B. Fåk, H. Godfrin, E. Krotscheck, H.-J. Lauter, T. Lichtenegger, J. Ollivier, and A. Sultan, *Phys. Rev. B* **94**, 024504 (2016).
- [118] D. K. Lee and F. J. Lee, *Phys. Rev. B* **11**, 4318 (1975).
- [119] L. P. Pitaevskii, *Zh. Eksp. Theor. Fiz.* **36**, 1168 (1959), [*Sov. Phys. JETP* **9**, 830 (1959)].
- [120] J. Wilks, *The Properties of Liquid and Solid Helium* (Clarendon, New York, Oxford, 1967).
- [121] S. A. Chin and E. Krotscheck, *Phys. Rev. B* **45**, 852 (1992).
- [122] S. A. Chin and E. Krotscheck, *Phys. Rev. Lett.* **65**, 2658 (1990).
- [123] S. A. Chin and E. Krotscheck, *Chem. Phys. Lett.* **178**, 435 (1991).
- [124] E. Krotscheck and R. Zillich, *J. Chem. Phys.* **115**, 10161 (2001).